

Properties of Various Malleable Iron Powder Grades

François Chagnon, Julie Campbell-Tremblay and Maryam Moravej

Rio Tinto Metal Powders
1655 Marie-Victorin
Sorel-Tracy
Quebec, Canada
J3R 4R4

francois.chagnon@riotinto.com; julie.campbell-tremblay@riotinto.com; maryam.moravej@riotinto.com

ABSTRACT

A novel powder grade has been developed to compete with ductile iron casting materials. This new malleable iron powder, MIP, is an iron-graphite composite powder in which the carbon is dispersed as graphite nodules in a ferritic matrix. MIP-A achieves almost 100% densification through liquid phase sintering with a sintered density of 7.5 g/cm³. Fatigue resistance can be improved by modifying the graphite clusters from a flaky shape in MIP-A to nodular in MIP-B. Also, by addition of ferromanganese (MIP-C) a significant improvement in hardenability can be achieved. This paper describes the properties of three materials, MIP-A, MIP-B and MIP-C, where the latter was developed to improve hardenability and make this material more appropriate for heat treatment.

INTRODUCTION

Supersolidus liquid phase sintering (SLPS) makes it possible to reach full density during the sintering cycle. This process involves prealloyed powders that, when heated to an intermediate temperature between the solidus and liquidus, nucleate a liquid within each particle. The amount of liquid produced is a function of the alloy composition and sintering temperature. The individual particles partially melt and hence promote densification by capillary induced rearrangement [1-2].

It is possible to perform SLPS with the Fe-C system. However, because of the high concentration of carbon, a carbidic structure is produced on cooling and negatively affects the mechanical properties. These can be improved by a post-sintering heat treatment [3-4] but this also increases the production costs. To solve this problem, a new malleable iron powder grade has been developed to produce PM parts with sintered densities of 7.5 g/cm³ through SLPS [5]. This powder is produced by water atomization of a Fe-2C-1Si melt, submitted to a malleabilization heat treatment to produce a powder exhibiting a ferritic matrix with graphite nodules evenly distributed in the core and surface of the iron particles as shown in figure 1.

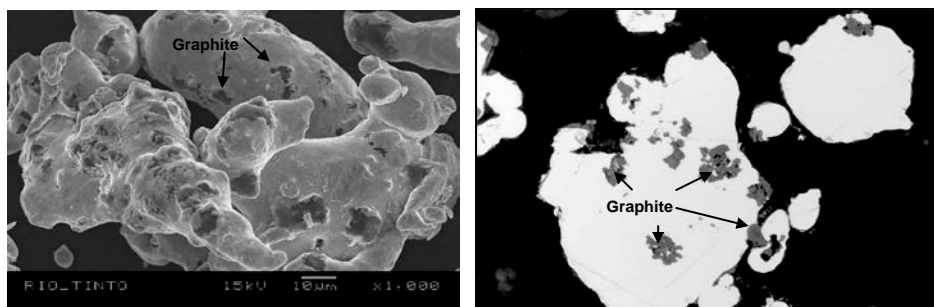


Figure 1. Particle shape and distribution of graphite nodules in MIP particles.

With the proper sintering profile, a pearlitic structure with a mixture of round and flaky graphite particles can be achieved. However, even if the presence of flaky graphite particles is not detrimental to the static properties, it has a negative effect on fatigue strength when the “nb flakes/mm² >100 μm” exceeds four [5]. Whereas parts made MIP-B cannot be heat treated due to the presence of phosphorus and MIP-A is not suitable for heat treatment of thick section sizes, a new MIP material, MIP-C, has been developed with addition of 0.5% Mn to promote hardenability.

The objective of this paper is to describe properties achieved after sintering and after heat treating specimens produced with the different MIP materials.

EXPERIMENTAL PROCEDURE

Table 1 shows the typical chemical and physical properties of MIP. Mixes with 0.75% wax were prepared with addition of ferrophosphorus or ferromanganese to reach the following compositions:

- MIP-A: MIP + 0.75% wax.
- MIP-B: MIP + 0.2%P + 0.75% wax
- MIP-C: MIP + 0.5% Mn + 0.75% wax.

Table 1. Chemical and physical properties of MIP.

C, %	O, %	Si, %	+250 μm , %	-250/+150 μm , %	-150/+45 μm , %	-45 μm , %	Apparent density, g/cm^3	Flow, s/50g
1.97	0.10	1.05	Trace	17	63	20	2.85	30

Rectangular bars (76.2 X 12.7 X 12.0 mm) and transverse rupture strength specimens (31.7X 12.7 X 6.4 mm) were pressed to 6.6 g/cm^3 and sintered during 10 minutes at either 1158 or 1166°C for MIP-A and C and for 30 minutes at either 1118 or 1124°C for MIP-B under a 90% N_2 /10% H_2 atmosphere. The special profiles required to successfully sinter MIP materials to full density are illustrated in figure 2.

The rectangular bars were machined to produce tensile specimens according to MPIF Standard 10. The bending fatigue strength was evaluated with transverse rupture strength specimens at a load ratio of $R=0.1$ and a run out limit of 2.5×10^6 cycles using the staircase method.

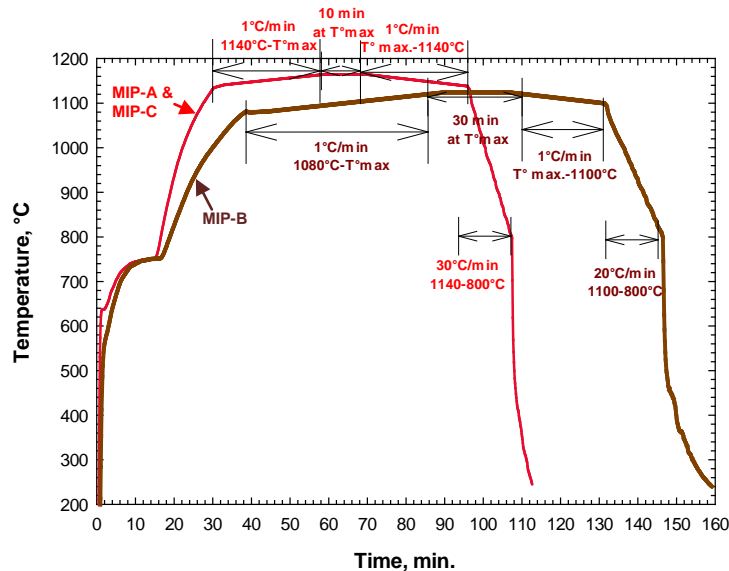


Figure 2. Temperature profiles used to sinter specimens pressed with MIP-A, MIP-B and MIP-C.

For the heat treatment, the specimens were austenitized for 30 minutes at 860°C, oil quenched at 60°C and tempered in the range of 150 to 600°C for 60 minutes. Retained austenite was quantified by X-ray analysis. Cylinders with an OD of 25.4 mm by 18.0 mm in height were also pressed to 6.6 g/cm^3 from MIP-A and MIP-C, sintered at 1166°C for 10 minutes, austenitized at 835°C and oil quenched. These were subsequently cut in half and hardness profiles were done on the cross section to compare the hardenability of both materials. Finally, the microstructure was evaluated by optical microscopy before and after Nital etching.

RESULTS AND DISCUSSION

Figure 3 compares the dimensional change and density values of the three materials sintered at both ends of their sintering windows. The liquid phase produced during sintering allows MIP materials to achieve almost 100% density. Because of the presence of free graphite in the structure, the maximum density that can be reached is about 7.60 g/cm^3 . Shrinkage increases with sintered density but levels off when reaching the sintering window of MIP materials, 1158-1166°C for MIP-A and C and 1118-1124 for MIP-B. Within their respective sintering windows, dimensional change variations within $\pm 0.1\%$ can be maintained for the various MIP materials.

Figure 4 compares the tensile properties, hardness and bending fatigue strength of MIP-A, B and C. The highest tensile and yield strength values, 900 and 590 MPa, are reached with MIP-C. This

material also shows the best elongation values and the highest hardness. The highest bending fatigue strength, 505 MPa, is observed with MIP-B.

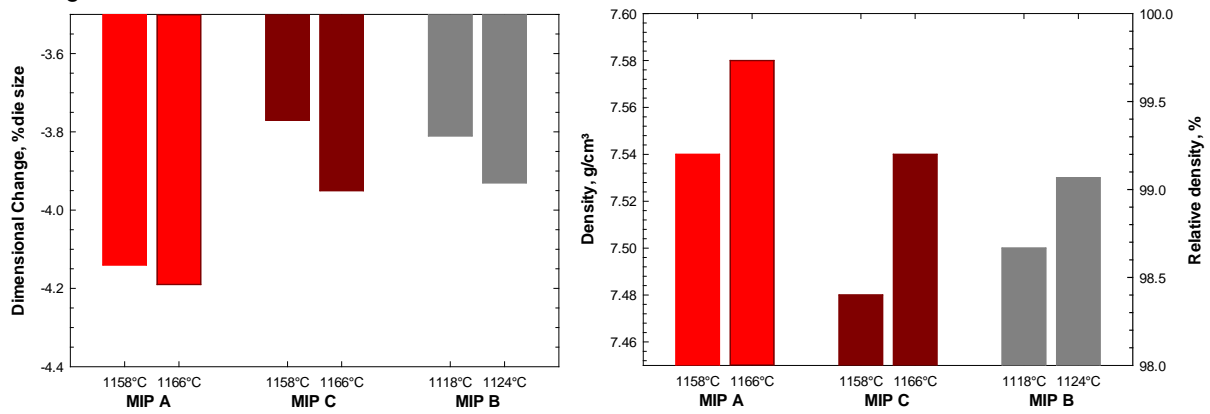


Figure 3. Effect of sintering temperature on dimensional change and density of bars made with MIP-A, MIP-B and MIP-C.

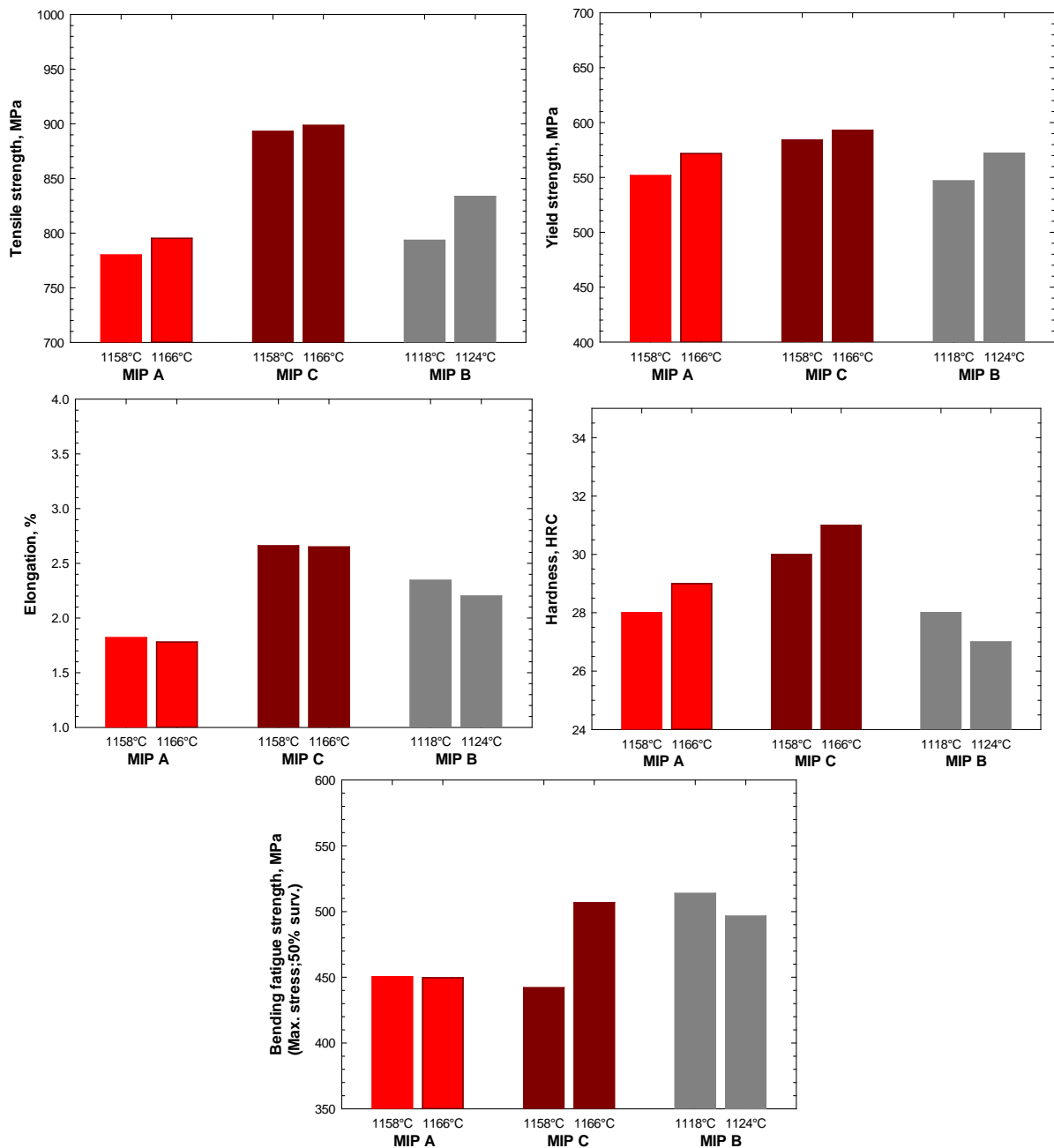


Figure 4. Effect of sintering temperature on tensile properties, hardness and bending fatigue strength of specimens made with MIP-A, MIP-B and MIP-C.

As shown in figure 5, MIP-B shows rounder graphite particle shape than MIP-A and MIP-C, which accounts for the high fatigue strength [6]. However, similar bending fatigue strength can be achieved with MIP-C when sintered at 1166°C, because of its higher density vs 1158°C and the presence of a very fine pearlitic structure. Indeed, fatigue strength of MIP materials is very sensitive to density and graphite shape. In a previous paper [5], it has been demonstrated that the presence of residual porosities with large and irregular shape of graphite particles are very detrimental to fatigue strength and sintering practices favoring pore agglomeration or over-sintering must be avoided. The fine pearlite observed with MIP-C also accounts for the highest tensile properties reached with this material.

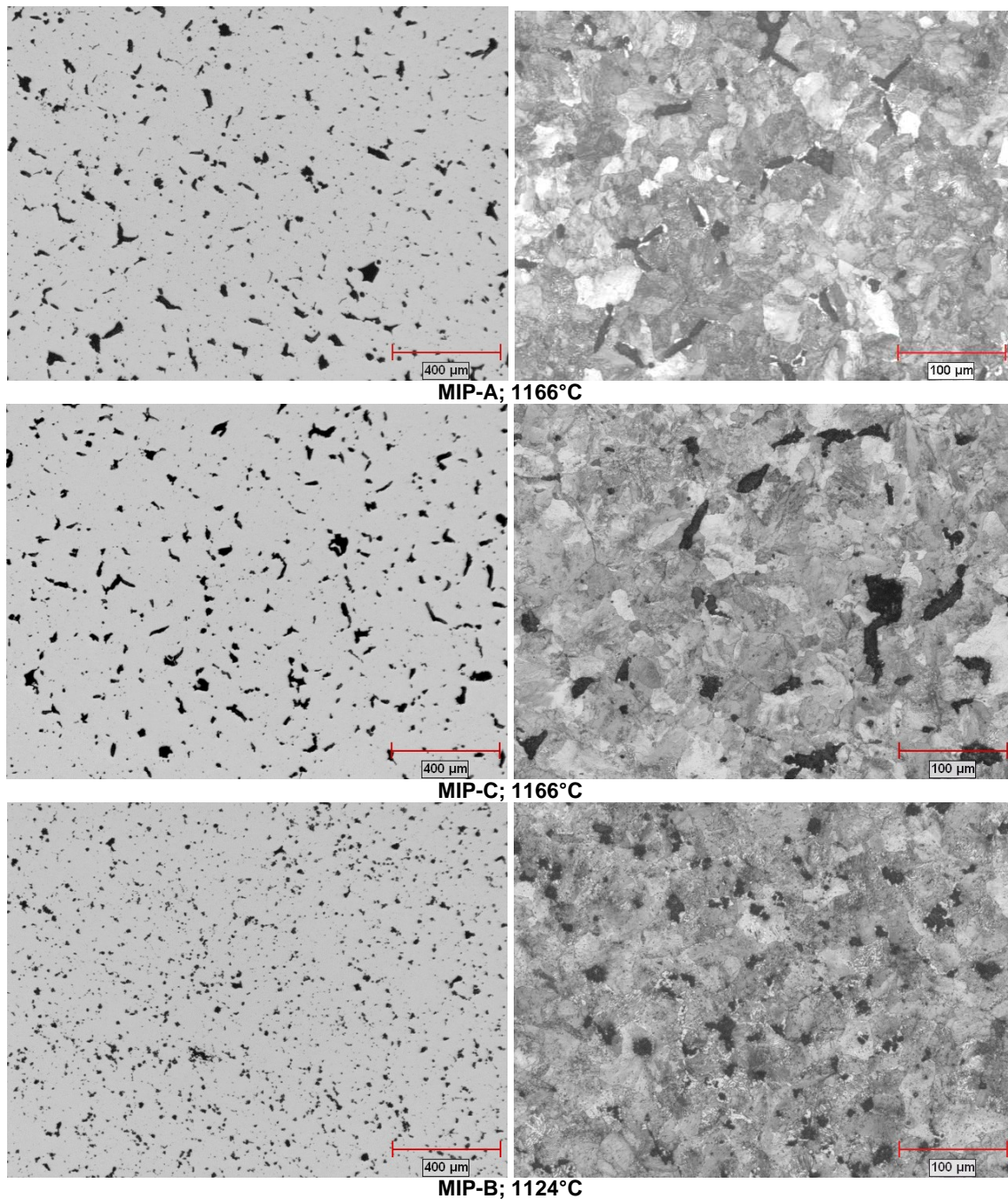


Figure 5. Microstructures before and after etching specimens made with MIP-A, MIP-C and MIP-B.

Figure 6 illustrates the hardness profiles on cross sections of cylinders made with MIP-A and MIP-C as well as the etched microstructures in the core of the specimens. It is worth noting these specimens were austenitized at a low temperature to promote differentiation between both materials. MIP-C

material achieves higher hardness values than MIP-A material. Also, for the latter material, hardness significantly decreases from the surface, 45 HRC, to the center of the specimen, 20 HRC while it decreases only from about 55 to 50 HRC for MIP-C. The corresponding microstructures in the core of the specimens is pearlitic for MIP-A and fully martensitic for MIP-C and reflects the increase in hardenability of MIP when 0.5% Mn is introduced in the alloy system.

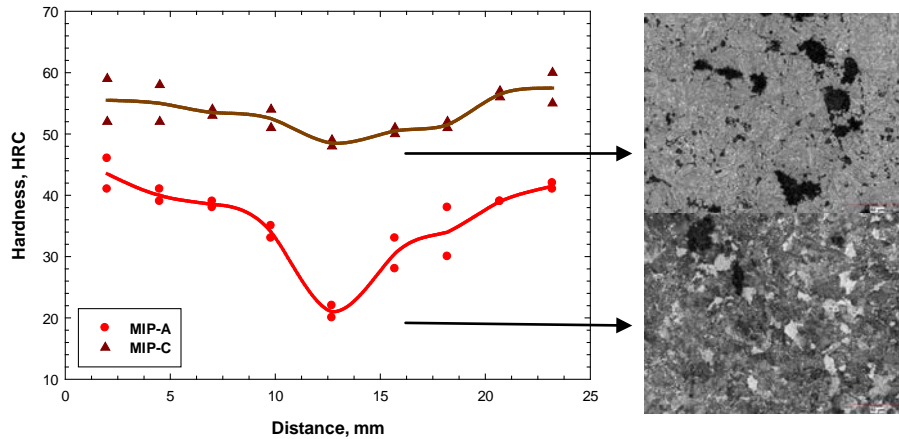


Figure 6. Hardness profiles carried out on the cross section of cylinders made with MIP-A and MIP-C after oil quench (no tempering).

Figure 7 illustrates the effect of tempering temperature on hardness of specimens pressed with MIP-C. Hardness only decreases from 60 HRC at 150°C to 55 HRC at 350°C and then quickly drops to 33 HRC at 550°C. About 35% retained austenite is present in the as-quenched specimens. However, it sharply decreases to 0% at a tempering temperature of 300°C.

Figure 8 illustrates the effect of tempering temperature on tensile and bending fatigue strength. None of the material exhibits any yield strength for tempering temperatures in the range of 225 to 425°C. The highest tensile strength is observed for a tempering temperature of 425°C, around 1350 MPa, while the highest bending fatigue strength, 550 MPa, is reached at 200°C. Therefore, from these results, retained austenite must be completely transformed to achieve high tensile strength while some amount, around 20% is required to improve fatigue strength. This has also been observed with sinterhardened PM steels [7]. Two mechanisms are proposed to explain the beneficial effect of retained austenite on fatigue performance [8]. Firstly, during fatigue stressing, some retained austenite is transformed into martensite, thus increasing fracture resistance. Secondly, when a crack encounters a soft retained austenite region, it is diverted and branched or blunted.

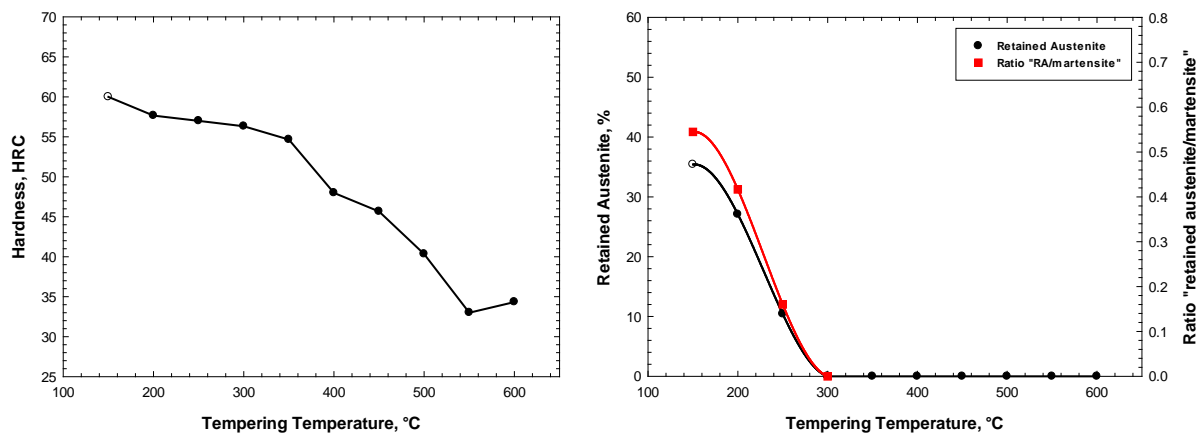


Figure 7. Variation of hardness and retained austenite with tempering temperature.

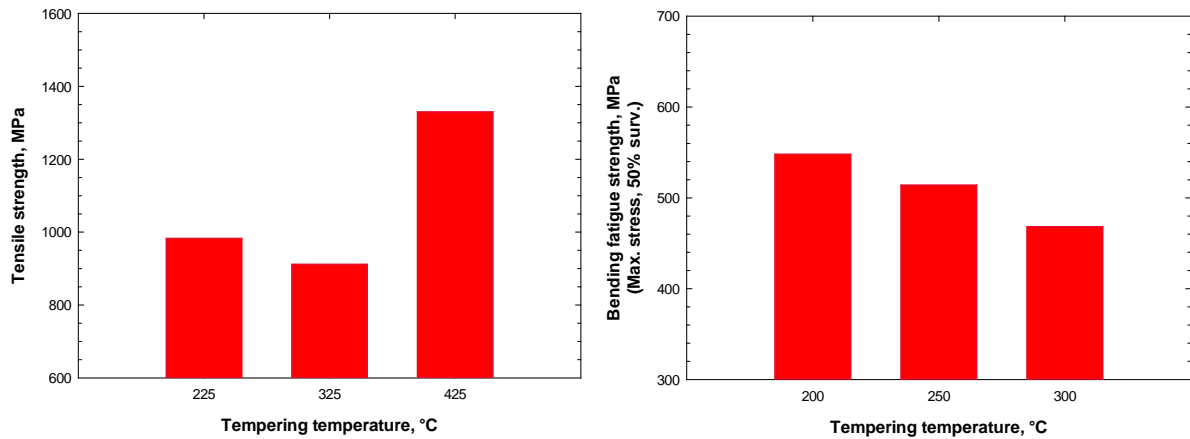


Figure 8. Effect of tempering temperature on tensile strength and bending fatigue strength.

CONCLUSIONS

- Three materials based on a new malleable iron powder grade have been developed for specific applications. These materials shrink to almost full density through liquid phase sintering and can maintain dimensional change tolerances of $\pm 0.1\%$ when sintered within their sintering windows.
- MIP-B achieves the best fatigue strength, 505 MPa, in the as-sintered condition due to the presence of round graphite nodules.
- MIP-C achieves the best tensile properties after sintering, 900 and 590 MPa for the tensile and yield strengths, due to the presence of 0.5% Mn which refines the pearlite.
- Addition of 0.5% Mn (MIP-C) significantly improves hardenability compared to MIP-A. Tensile strength of about 1350 MPa can be reached after oil quenching and tempering at 425°C.
- The best bending fatigue strength, 550 MPa at $R=0.1$, after quenching MIP-C specimens is reached at a tempering temperature of 200°C. About 20% retained austenite is present after tempering at this temperature.

REFERENCES

1. German, R.M.; "A Quantitative Theory for Supersolidus Liquid Phase Sintering", Powder Metallurgy, 1991, vol. 34, No. 2, pp 101-107.
2. German, R.M.; "Supersolidus Liquid Phase Sintering Part I; Process Review", The International Journal of Powder Metallurgy, American Powder Metallurgy Institute, Princeton, 1990, vol. 26, pp. 23-34.
3. Shivanath, R., Kucharski, K and Jones, P.; "Press and Sinter Process for High Density Components", US patent 6,346,213.
4. Young, E.; "High Density Supersolidus Liquid Phase Sintering of Steel Powders", M. Sc. Thesis, The University of British Columbia, 2001.
5. F. Chagnon and C. Coscia; "Development and Properties of a New Malleable Iron Powder Grade"; Advances in Powder Metallurgy & Particulate Materials; MPIF, Princeton, 2012, part 10, pp 7-20.
6. M. Moravej, F. Chagnon and J. Campbell-Tremblay; "Characterization of Mechanical Properties and Machining Performances of New Malleable Iron Powder Grades", Advances in Powder Metallurgy & Particulate Materials; MPIF, Princeton, 2012, part 10, pp 21-34.
7. F. Chagnon; "Effect of Sintering Temperature on Static and Dynamic Properties of Sinter Hardened Materials", Advances in Powder Metallurgy & Particulate Materials, MPIF, Princeton, 2009, Part 5, pp 52-64.
8. A.Kumar Sinha; "Ferrous Physical Metallurgy", Butterworth Publishers, Boston, 1989, pp 324-325.